An Analysis of the Visible Absorption Spectrum of Chlorophyll a Monomer, Dimer, and Oligomers in Solution[1]

Lester L. Shipman, Therese M. Cotton,[2] James R. Norris, and Joseph J. Katz*

Contribution from the Chemistry Division, Argonne National Laboratory, Argonne, Illinois 60439. *Received May 3, 1976*

Abstract: The visible absorption spectra of chlorophyll a monomer, dimer, and oligomers in solution have been analyzed with respect to peak positions, extinction coefficients, oscillator strengths, and dipole strengths. Exciton theory has been used to relate features in the dimer and oligomer spectra to features in the monomer spectrum. Conversion from penta- to hexacoordination at Mg strongly red shifts the Q_x transition so that $Q_x(0,0)$ appears between $Q_y(0,0)$ and $Q_y(0,1)$. The relative bulk solvent environmental shifts of the Q_y transition in carbon tetrachloride and *n*-octane have been computed. Because chlorophyll a oligomers have absorption spectra strikingly similar to antenna chlorophyll in green plants, oligomeric chlorophyll a is proposed as a model for antenna chlorophyll.

I. Introduction

Chlorophyll (Chl) molecules perform several important roles during the primary events of photosynthesis that are generally believed to occur within photosynthetic units.[3-5] In particular, hundreds of Chl molecules (generally referred to as antenna Chl) act cooperatively to harvest (absorb) light quanta, and thereby undergo excitation to excited singlet electronic states. This excitation energy is then transferred very efficiently to a few special[6] Chl molecules constituting a photoreaction center[7] (i.e., trap) where the electronic excitation energy is converted into chemical oxidizing and reducing capacity. A detailed knowledge of the light-absorptive and energy-transfer properties of interacting Chl molecules is essential for a thorough understanding of the primary events of photosynthesis. Chl a (Figure 1), with which this paper is concerned, is the principal photoreceptor in the photosynthetic units of all organisms that carry out photosynthesis with the evolution of molecular oxygen.

The visible absorption spectrum of Chl a has been studied for more than 40 years,[8] and during that period an extensive literature has accumulated on the subject. It is outside the scope of this paper to review that body of literature: fortunately, several reviews of portions of this literature already are available.[6,9-16] Of particular importance to our present discussion is the electron donor-acceptor properties of Chl a. Chl a forms self-aggregates and Chl a-ligand adducts via electron donor-acceptor interactions with Mg as acceptor for ring V keto C=O (in the case of self-aggregates) or ligand (for the case of Chl a-ligand adducts) lone-pair electrons.[12] The Mg is usually pentacoordinated but may become hexacoordinated under forcing conditions.[12]

In the present study the visible absorption spectra of Chl a monomer, dimer, and oligomers in solution have been analyzed with respect to peak positions, extinction coefficients, oscillator strengths, and dipole strengths. A recently derived[17] exciton formulation for molecular aggregates has been used to relate features in the dimer and oligomer absorption spectra to features in the absorption spectrum of the monomer. The effects of five vs. six coordination at Mg on the visible absorption spectrum have been delineated, with the result that the coordination state of the Mg in Chl a can be deduced from the visible spectra.

II. Experimental Section

Chl a was prepared by the method of Strain and Svec.[18] Additional purification of the Chl a was obtained by rechromatographing the samples on powdered sugar, retaining only the central portion of the Chl a zone. It should be noted that our Chl a samples contain a variable content of the diastereoisomeric Chl a′, which differs from Chl a by having the opposite configuration (i.e., H and $-CO_2CH_3$ are interchanged) at position 10 (Figure 1). When Chl a is dissolved in basic solvents, enolization in ring V leads to the rapid formation of the equilibrium mixture of diastereoisomers. The visible absorption spectra of Chl a and Chl a′ are essentially identical,[19] and for the particular systems described here we believe that the spectral observations are not significantly affected by the presence of the equilibrium between diastereoisomers. Pheophytin a was prepared by treatment of Chl a with a dilute solution of HCl in diethyl ether. $Eu(fod)_3$, tris(1,1,1,2,2,3,3-heptafluoro-7,7-dimethyl-4,6-octanedionato)europium, was obtained from the Norell Chemical Company. Solvents used were carbon tetrachloride (Mallinckrodt; analytical grade), pyridine (Burdick and Jackson; distilled in glass), anhydrous diethyl ether (Mallinckrodt; analytical grade), and *n*-octane (Chemical Samples; 99% purity).

The Chl a samples were thoroughly dried by codistillation three times with dry CCl_4 and then heating the Chl a at 60 °C for 30 min under vacuum ($\sim 10^{-5}$ mm). Solvents were thoroughly dried before use by the following procedure. 3 Å Linde molecular sieves were activated by heating for a minimum of 24 h at 350 °C. These sieves were then evacuated on a vacuum line while still hot. Solvents were dried over the sieves for at least 24 h, degassed on a vacuum line, and distilled onto fresh degassed sieves. Following this drying procedure, neither the Chl a samples nor the solvents were subsequently exposed to ordinary air.

For the preparation of stock solutions, Chl a samples weighing a few milligrams were weighed out on a Mettler microbalance to the nearest 10 μg and then transferred to a volumetric flask containing dry solvent. All glassware was dried at high temperature and inserted into a drybox while still warm. All dilutions were performed with dry Hamilton microliter syringes. For those experiments where bases were added to disaggregate Chl a dimers or oligomers, known quantities of base were measured out with Hamilton microliter syringes. All stock solution preparation, dilutions, and other manipulations were performed in a deoxidized N_2-purged drybox.

Absorption spectra and baselines were recorded on a Cary 14 spectrophotometer equipped with a digitizer interfaced to the ANL Chemistry Division's Sigma 5 computer where the digitized data were stored prior to deconvolution. The Cary 14-digitizer combination was checked for accuracy against NBS Standard Reference 930b (glass filters) and was found to be accurate to within a few thousandths of an optical density unit over the spectral range of interest in this study.

III. Computer Deconvolution of Spectra

The visible absorption spectra and baselines taken in the present study were digitized and stored (on peripheral storage

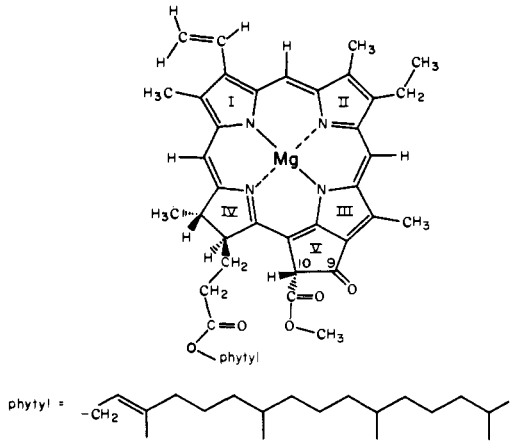

Figure 1. Chemical structure of chlorophyll a.

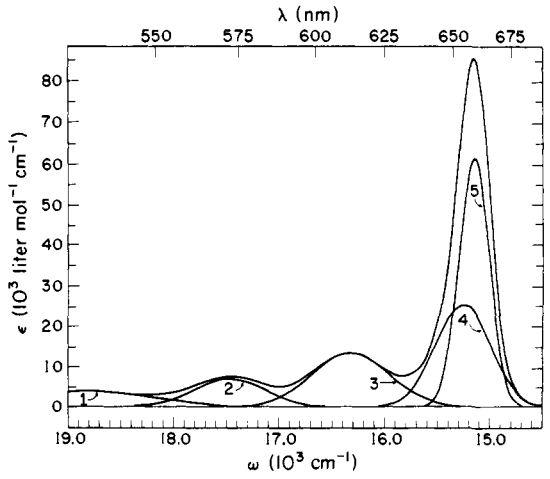

Figure 2. Visible absorption spectrum of 10^{-5} M chlorophyll a-diethyl ether in diethyl ether.

on the Chemistry Division's Sigma 5 computing system) as recorded. Later the digitized spectra and baselines were recalled from storage, the baseline was subtracted from the absorption spectrum to give a baseline-corrected absorption spectrum, and then the baseline-corrected absorption spectrum was computer deconvoluted using Gaussian components. The functional form of a Gaussian component is given by

$$\epsilon(\omega) = \epsilon_0 \exp\{-\tfrac{1}{2}[(\omega - \omega_0)/\delta]^2\} \qquad (1)$$

where ϵ (l. mol^{-1} cm^{-1}) is the extinction coefficient, ϵ_0 (l. mol^{-1} cm^{-1}) is the height of the Gaussian at the maximum, ω (cm^{-1}) is the energy, ω_0 (cm^{-1}) is the position of the maximum, and δ (cm^{-1}) is the Gaussian standard deviation, a measure of the width of the Gaussian component. The parameters ϵ_0, ω_0, and δ were determined by a computer program C-151, Argonne Program Library, which was adapted by A. Zielen for the ANL Chemistry Division's Sigma 5 computing system. This deconvolution program utilizes the variable metric minimization procedure of Davidon[20] to obtain a best least-squares fit of the computed spectrum (i.e., the sum of the Gaussian components) to the digitized experimental spectrum. Input to the program consists of the digitized spectrum (data points every 2 Å), the digitized baseline, the total number of Gaussian components to be used in the fit, and initial estimates for the Gaussian parameters. We were routinely able to obtain fits that matched the experimental spectra with root-mean-square errors of less than 0.002 optical density units. We purposely held the number of Gaussians down to the minimum number required to obtain fits with root-mean-square errors of less than 0.002 optical density units. It should be noted that this fitting procedure does not guarantee that a unique fit will be obtained. Although the spectra were recorded by wavelength (nm), the digitized spectra were converted to energy (cm^{-1}) before deconvolution.

IV. Exciton Theory

Exciton theory is a quantum mechanical formalism by which to express the electronic states of an assemblage (aggregate, crystal, etc.) of molecules from the electronic states of the component monomers. A first-order exciton theory for Chl aggregates has recently appeared;[17] this formalism, unlike previous exciton formalisms that have been applied to Chl aggregates, takes environmental shifts of transition energies explicitly into account. Because this exciton formalism has been described in detail elsewhere,[17] the details are not repeated here. In the present study we used exciton theory to establish the relationships between features in the visible absorption spectrum of monomeric Chl a and features in the visible absorption spectra of dimeric and oligomeric Chl a.

Table I. Positions and Heights of Maxima in the Visible Absorption Spectrum of Chl a-Diethyl Ether in Diethyl Ether and $(Chl\ a)_2$ in Carbon Tetrachloride

Chl a-diethyl ether in diethyl ether		$(Chl\ a)_2$ in carbon tetrachloride	
Positions[a] of maxima	Heights[b] of maxima	Positions[a] of maxima	Heights[b] of maxima
18.86 (530)	3.8	18.60 (538)	3.4
17.40 (575)	7.1	17.02 (588)	9.0
16.31 (613)	13.0	15.96 (627)	17.2
15.17 (659)	84.9	14.94 (669)	55.7

[a] Units are 10^3 cm^{-1} (nm in parentheses). [b] Units are 10^3 l. mol^{-1} cm^{-1}.

V. Visible Absorption Spectrum of Chlorophyll a Monomer

Let S_0, S_1, and S_2 denote the ground electronic state, first excited singlet electronic state, and second excited singlet electronic state, respectively, of Chl a. The visible absorption spectrum (Figure 2) of Chl a monomer in the red and orange regions of the visible absorption spectrum is due primarily to the $S_0 \rightarrow S_1$ transition, also called the Q_y transition. Similarly, the absorption spectrum in the green and yellow regions is due primarily to the $S_0 \rightarrow S_2$ transition, also called the Q_x transition. The oscillator strength of the Q_y transition is over five times greater than the oscillator strength of the Q_x transition. The transition dipole for the Q_y transition is directed approximately along the N(I)-N(III) axis (Figure 1) and the transition dipole for the Q_x transition is directed approximately along the N(II)-N(IV) axis (Figure 1).[21] The $S_0 \rightarrow S_n$ $n > 2$ transitions are located in the blue and higher energy regions of the absorption spectrum. *Only* the Q_y and Q_x transitions have been analyzed in the present study.

A. Pentacoordinate Chlorophyll a Monomer. The peak positions and maximum extinction coefficients for 10^{-5} M Chl a-diethyl ether in diethyl ether are given in Table I. The Q_y and Q_x transitions are each split into at least two discrete vibronic peaks at 659 nm [$Q_y(0,0)$], 613 nm [$Q_y(0,1)$], 575 nm [$Q_x(0,0)$ and $Q_y(0,2)$], and 530 nm [$Q_x(0,1)$]; the energy spacing between $Q_y(0,0)$ and $Q_y(0,1)$ is 1.14×10^3 cm^{-1}. The averaged results from several runs of recording and deconvoluting the visible absorption spectra of 10^{-5} M Chl a-diethyl ether are given in Table II. The Gaussian parameters (ϵ_0, ω_0, and δ) as defined in eq 1, the oscillator strengths[22] (f) and dipole strengths[22] are given for each Gaussian component in Table II. The numbering of the Gaussian components in Table

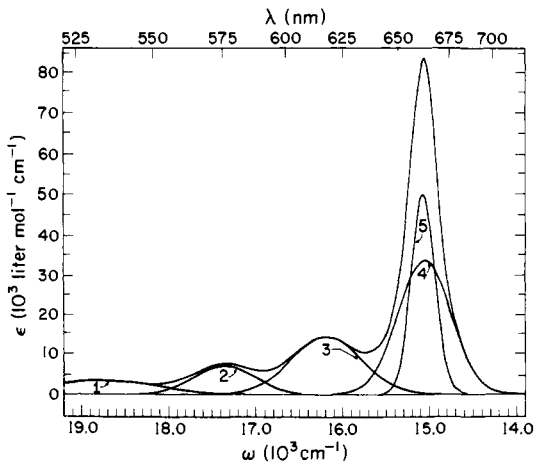

Figure 3. Visible absorption spectrum of 10^{-5} M chlorophyll a-diethyl ether in carbon tetrachloride.

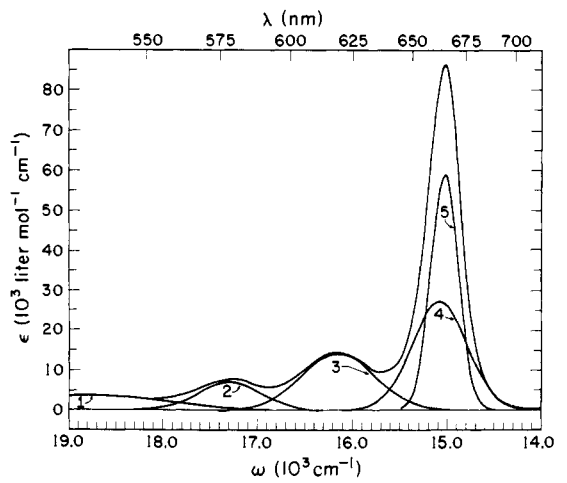

Figure 4. Visible absorption spectrum of 10^{-5} M chlorophyll a-Pyr in carbon tetrachloride.

Table II. Gaussian Deconvolution of the Low-Energy Band in the Visible Absorption Spectrum of Chl a-Diethyl Ether in Diethyl Ether[a]

Gaussian number	ϵ_0[b]	ω_0[c]	δ[d]	f[e]	Dipole strength[f]
1	3.6	18.85 (530)	0.629	0.018	2.1
2	6.7	17.47 (572)	0.330	0.018	2.1
3	13.0	16.32 (613)	0.373	0.038	5.0
4	25.8	15.26 (655)	0.253	0.052	7.2
5	60.2	15.16 (660)	0.141	0.068	9.5

[a] $\epsilon(\omega) = \epsilon_0 \exp\{-\frac{1}{2}[(\omega - \omega_0)/\delta]^2\}$. [b] Height at Gaussian maximum; units are 10^3 l. mol^{-1} cm^{-1}. [c] Position of Gaussian maximum; units are 10^3 cm^{-1} (nanometers in parentheses). [d] Gaussian standard deviation; units are 10^3 cm^{-1}. [e] Oscillator strength; unitless, see footnote 22. [f] Units are (Debyes)^2, see footnote 22.

II corresponds to the numbering of the Gaussian components in Figure 2. Except for the red-most (and largest) peak, all the peaks in the spectrum can be deconvoluted with a single Gaussian (Figure 2). The largest peak requires the sum of a narrow ($\delta \simeq 141$ cm^{-1}) component and a broad ($\delta \simeq 253$ cm^{-1}) component at slightly higher energy. This need for a two-component fit may reflect the coupling of the Q_y transition to more than one normal vibrational mode. Most of the splitting into vibronic peaks can be accounted for by assuming that the Q_y transition is coupled to one or more C⋯C and C⋯N stretching normal modes of frequency near 1140 cm^{-1}; however, the broadening of the largest peak toward higher energy may reflect the coupling of the Q_y transition to one or more normal modes involving Mg motions. A recent vibrationally resolved low-temperature fluorescence spectrum[23] of Chl a does indicate considerable vibronic structure in the low-frequency range. We have chosen to deconvolute the absorption spectrum in energy units (cm^{-1}) rather than wavelength units (nm); however, for the peak widths and positions involved, essentially identical results are found by either deconvolution. The Gaussian at 572 nm was separated into $Q_y(0,2)$ and $Q_x(0,0)$ contributions by making the approximation that the Q_y transition is coupled to only one normal vibrational mode and then applying the vibrational overlap formulas of Siebrand[24] to calculate the dipole strength of $Q_y(0,2)$ from the dipole strengths of $Q_y(0,0)$ and $Q_y(0,1)$. This computational procedure gives an estimate of 0.7 D^2 for the dipole strength of $Q_y(0,2)$. The total dipole strengths are 9.5 + 7.2 + 5.0 + 0.7 = 22.4 D^2 and 2.1 + 1.4 = 3.5 D^2 for the Q_y and Q_x transitions, respectively. The corresponding total oscillator strengths are 0.068 + 0.052 + 0.038 + 0.006 = 0.164 and 0.018 + 0.012 = 0.030, respectively.

It is of interest to know how the various ligands coordinated to Mg and the bulk solvent affect the peak positions and dipole strengths of the transitions. We have taken the approach of titrating $(\text{Chl a})_2$ in carbon tetrachloride (nominal[25] Chl a concentration $\sim 10^{-5}$ M) with either diethyl ether or pyridine until the dimer is essentially disaggregated to monomer (Chl a-diethyl ether or Chl a-Pyr, respectively). The disappearance of dimer was followed by the disappearance of the ~680 nm shoulder in the absorption spectrum associated with the dimer. The resulting monomer spectra were recorded and deconvoluted (Figures 3 and 4). The position of the major red peak shifts from 659 nm (15.17×10^3 cm^{-1}) for Chl a-diethyl ether in diethyl ether solution to 664 nm (15.07×10^3 cm^{-1}) for Chl a-diethyl ether in CCl_4 and 665 nm (15.03×10^3 cm^{-1}) for Chl a-Pyr in CCl_4. The dipole strengths of Q_y and Q_x for both Chl a-diethyl ether and Chl a-Pyr in carbon tetrachloride are approximately 23 and 3 D^2, respectively.

B. Hexacoordinate Chlorophyll a Monomer. The monomer spectra discussed in the last section are all spectra of predominantly pentacoordinated chlorophyll a monomer with four of the Mg coordination sites being the four pyrrole nitrogens and a fifth coordination site (i.e., an axial site) being occupied by pyridine or diethyl ether. Presumably, the Mg is displaced approximately 0.4 Å out of the plane of the macrocycle[26] toward the ligand in a square-pyramidal geometry at Mg. It is of interest to know what changes in the spectrum are brought about by the conversion from pentacoordination to hexacoordination where geometry at Mg is presumably octahedral and the Mg lies more or less in the macrocycle plane. The most pronounced spectral change in the conversion from penta- to hexacoordination is the strong red shift of the Q_x transition relative to the Q_y transition so that the $Q_x(0,0)$ peak appears at a position intermediate between the $Q_y(0,0)$ and $Q_y(0,1)$ peaks. Evans and Katz[27] have studied the Q_x red shift for bacteriochlorophyll a (Bchl a) by titrating Bchl a in toluene with pyridine. They concluded that the equilibrium constant (K) for the conversion

$$\text{Bchl·Pyr} + \text{Pyr} \overset{K}{\rightleftharpoons} \text{Bchl·Pyr}_2 \qquad (2)$$

is 11 l./mol in toluene at room temperature. We expect that a similar value for the equilibrium constant holds for the conversion of Chl a-Pyr to Chl a-Pyr_2. Thus, for pyridine as the bulk solvent ([Pyr] = 12.4 M) and under conditions such that the nominal[25] Chl a concentration is much less than 12.4 M,

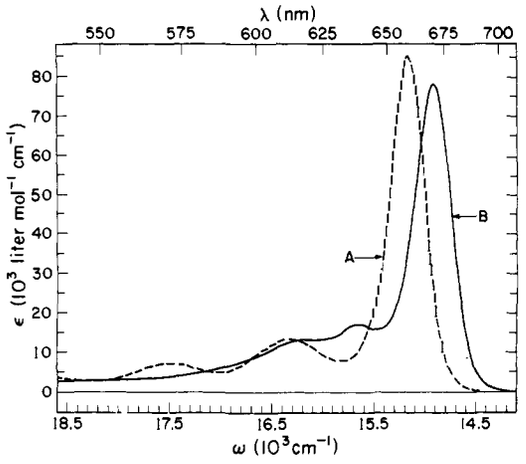

Figure 5. Visible absorption spectra of 10^{-5} M Chl a-diethyl ether in diethyl ether (spectrum A) and 10^{-5} M Chl a·Pyr_2 in pyridine (spectrum B).

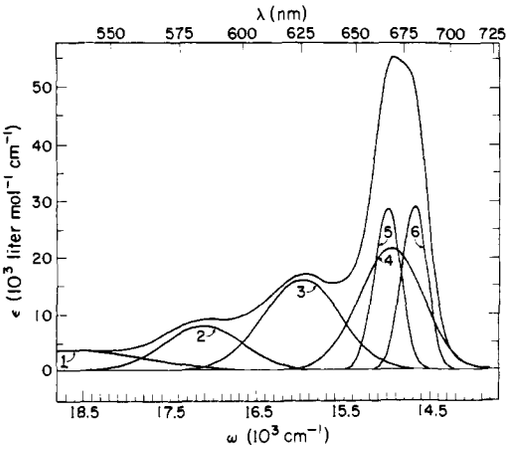

Figure 6. Visible absorption spectrum of chlorophyll a dimer in carbon tetrachloride at a nominal[25] chlorophyll a concentration of 10^{-5} M.

over 99% of the Chl a will be present as the disolvate species, Chl a·Pyr_2. The spectrum of Chl a-diethyl ether in diethyl ether (dashed line) and Chl a·Pyr_2 in pyridine (solid line) are shown in Figure 5. The entire absorption spectrum has been red-shifted in bulk solvent pyridine compared with bulk solvent diethyl ether, and the Q_x transition has been red-shifted farther than the Q_y transition. Specifically, $Q_y(0,0)$ has shifted from 659 to 670 nm, and $Q_x(0,0)$ has shifted from 575 to 639 nm. We point out that McCartin,[28] Seely and Jensen,[29] and Cotton et al.[14] have previously observed this peak at 639 nm for Chl a in dry pyridine. Cotton et al.[14] found that the peak at 639 nm disappeared in wet pyridine. The entire spectrum is not as red-shifted with toluene as the bulk solvent as it is with pyridine as the bulk solvent; in this regard Evans and Katz[27] have observed the appearance of a peak at 633 nm between $Q_y(0,0)$ and $Q_y(0,1)$ when titrating Chl a with pyridine in bulk solvent toluene. Pyridine is not the only nucleophile that will form hexacoordinate Chl a species at room temperature. For example, Seely and Jensen[29] and Cotton et al.[14] have reported peaks near 629 nm for Chl a in tetrahydrofuran and Seely and Jensen[29] have reported a peak at 623 nm in dioxane.

Lower temperatures definitely favor the formation of the hexacoordinate species over the pentacoordinate species. While Chl a in diethyl ether is largely the pentacoordinate species at room temperature, the hexacoordinate species is found at low temperature. Song[30] has observed a peak between the $Q_y(0,0)$ and $Q_y(0,1)$ peaks in the fluorescence excitation spectrum of Chl a in diethyl ether at 77 K. Song[30] has also found that the fluorescence polarization spectrum indicates that the former peak [i.e., $Q_x(0,0)$] is polarized differently from the latter two peaks [i.e., $Q_y(0,0)$ and $Q_y(0,1)$]. Freed and Sancier[31] have reported a peak at 638 nm between the $Q_y(0,0)$ and $Q_y(0,1)$ peaks for Chl a in the solvent system composed of 20% *n*-propyl ether, 40% propane, and 40% propene by volume at 75 K. Sevchenko et al.[32] have observed the appearance of a peak (~635 nm) between the $Q_y(0,0)$ and $Q_y(0,1)$ peaks in an ethanol glass at 77 K, and their fluorescence polarization spectrum indicates that this intermediate transition is polarized differently from the $Q_y(0,0)$ and $Q_y(0,1)$ peaks; this supports the assignment of the intermediate peak as $Q_x(0,0)$. A word of caution in regard to the assignment of the spectrum of the hexacoordinate species is in order. Song[30] has observed a small emission peak between the (0,0) and (1,0) vibronic peaks in the $S_1 \rightarrow S_0$ fluorescence spectrum of Chl a at 15 K in diethyl ether. The appearance of this peak in the emission spectrum suggests that some of the peak between the $Q_y(0,0)$ and $Q_y(0,1)$ peaks in the fluorescence excitation spectrum of this system may be due to a vibronic component of Q_y.

Table III. Gaussian Deconvolution of the Low-Energy Band in the Visible Absorption Spectrum of $(Chl\ a)_2$ in Carbon Tetrachloride[a]

Gaussian number	ϵ_0[b]	ω_0[c]	δ[d]	f[e]	Dipole strength[f]
1	3.3	18.57 (539)	0.694	0.016	1.9
2	7.9	17.12 (584)	0.453	0.027	3.3
3	15.7	15.99 (625)	0.436	0.050	6.8
4	21.0	14.97 (668)	0.378	0.058	8.3
5	29.5	15.00 (667)	0.156	0.034	4.8
6	28.5	14.69 (681)	0.145	0.031	4.4

[a] $\epsilon(\omega) = \epsilon_0 \exp\{-\frac{1}{2}[(\omega - \omega_0)/\delta]^2\}$. [b] Height at Gaussian maximum; units are 10^3 l. mol^{-1} cm^{-1}. [c] Position at Gaussian maximum; units are 10^3 cm^{-1} (nanometers in parentheses). [d] Gaussian standard deviation; units are 10^3 cm^{-1}. [e] Oscillator strength; unitless, see footnote 22. [f] Units are $(Debyes)^2$, see footnote 22.

VI. Visible Absorption Spectrum of Chlorophyll a Dimer

From vapor phase osmometry[33] it is known that in the absence of adventitious nucleophiles Chl a exists in dimeric form in CCl_4. The strongest and most direct evidence for the structure of $(Chl\ a)_2$ in carbon tetrachloride has come from infrared[34-36] and ^{13}C NMR spectroscopic studies.[37-39] The extensive experimental evidence along with the arguments leading to the accepted dimer structure have been reviewed elsewhere[16] and thus need not be repeated here. The Chl a molecules in the dimer are bound together through the coordination interaction of the ring V keto C=O at position 9 (Figure 1) of one Chl a molecule (i.e., the donor) to the Mg of the second Chl a molecule (i.e., the acceptor). The structure is dynamic such that the two Chl a molecules are interchanging donor and acceptor roles much faster than the NMR time scale but much slower than the time scale of a C=O stretching vibration ($\sim 2 \times 10^{-14}$ s). The tilt of one macrocycle plane relative to the other has not been determined accurately, but it is reasonable to expect that the two macrocycle planes tend to align perpendicular so as to optimize the directionality of the keto C=O···Mg coordination bond and minimize overlap repulsions.

The visible absorption spectrum of 10^{-5} M (nominal[25] concentration) Chl a in CCl_4 is shown in Figure 6. The numbering of the Gaussians in Figure 6 is the same as the numbering in Table III where the Gaussian parameters, oscillator strengths, and dipole strengths are given. The peak positions and peak heights in the dimer spectrum are summarized in Table I. We assume that all of Gaussian 1 and two-thirds of

Gaussian 2 may be assigned to the Q_x transitions and Gaussians 3-6 and one-third of Gaussian 2 may be assigned to the Q_y transitions (Figure 6). Under this assumption, the total dipole strengths for the Q_x and Q_y transitions are 1.9 + 2.2 = 4.1 D^2 and 6.8 + 8.3 + 4.8 + 4.4 + 1.1 = 25.4 D^2, respectively. Overall (Q_x + Q_y) the dipole strength of (Chl a)$_2$ in CCl_4 is enhanced by 14% over the dipole strength of Chl a·diethyl etherate in diethyl ether and by 13% over Chl a·Pyr or Chl a·diethyl ether in CCl_4. Thus, Chl a- - -Chl a coordination interactions affect the dipole strength of Chl a.

Gaussians 5 and 6 (widths 156 and 145 cm^{-1}) in the dimer spectrum (Figure 6 and Table III) are related to Gaussian 5 (width 141 cm^{-1}) in the monomer spectrum (Figure 2 and Table II). The heights of Gaussians 5 and 6 (29.5 and 28.5 × 10^3 l. mol^{-1} cm^{-1}, respectively) in the dimer spectrum are approximately one-half the height of Gaussian 5 (60.2 × 10^3 l. mol^{-1} cm^{-1}) in the monomer spectrum if computed using the nominal[25] Chl a concentration. In all our figures we have used the nominal[25] Chl a concentrations, and therefore our extinction coefficients are actually in units of l. (mol of monomer)$^{-1}$ cm^{-1}. The dipole strengths of Gaussians 5 and 6 in the dimer spectrum are 4.8 and 4.4 D^2, respectively. We conclude that the two Q_y(0,0) transitions on the isolated monomer Chl a molecules interact to give two exciton transitions in the dimer and that these two exciton transitions have nearly equal dipole strength. The splitting of the two exciton transitions is 3.1 × 10^2 cm^{-1} (the separation between the positions of Gaussians 5 and 6), and the average position of the exciton transitions is 14.84 × 10^3 cm^{-1} (674 nm).

We note that the position (15.00 × 10^3 cm^{-1}) of Gaussian 5 in the dimer spectrum is very nearly the same as the position (15.02 × 10^3 cm^{-1}) of the corresponding Gaussian (i.e., Gaussian 5 in Figure 4) in the spectrum of Chl a·Pyr in CCl_4. The observations discussed above are used along with exciton theory in the next section to draw conclusions as to the nature of the exciton states in (Chl a)$_2$.

A. Exciton Theory: Chlorophyll a Dimer. In order to apply exciton theory[17] to Chl a dimer several symbols need be defined at the outset. Let Δ be the $S_0 \rightarrow S_1$ (Q_y) transition energy for an isolated Chl a monomer, σ_D be the environmental shift of the Q_y transition energy for a donor molecule in (Chl a)$_2$ in CCl_4, σ_A be the environmental shift of the Q_y transition energy for an acceptor Chl a molecule in (Chl a)$_2$ in CCl_4, and T be the transition density-transition density interaction energy between the Q_y transition density on the donor molecule and the Q_y transition density on the acceptor molecule. The exciton transition energies (ϵ_+ = 15.00 × 10^3 cm^{-1} and ϵ_- = 14.69 × 10^3 cm^{-1}) are then[17]

$$\epsilon_\pm = \Delta + \left(\frac{\sigma_A + \sigma_D}{2}\right) \pm \tfrac{1}{2}[(\sigma_A - \sigma_D)^2 + 4T^2]^{1/2} \quad (3)$$

The average transition energy (14.84 × 10^3 cm^{-1}) is given by

$$\frac{\epsilon_+ + \epsilon_-}{2} = \Delta + \frac{\sigma_A + \sigma_D}{2} \quad (4)$$

and the transition energy splitting (3.1 × 10^2 cm^{-1}) is given by

$$\epsilon_+ - \epsilon_- = [(\sigma_A - \sigma_D)^2 + 4T^2]^{1/2} \quad (5)$$

Because a Chl a molecule serves in an acceptor capacity both in the monomer species Chl a·Pyr and as the acceptor molecule in the dimeric species (Chl a)$_2$, and $\Delta + \sigma_A$ in monomeric pentacoordinate Chl a is nearly independent of ligand (compare the positions of the Q_y(0,0) peak for Chl a·diethyl ether and Chl a·Pyr in bulk solvent CCl_4 in section V.A.), it is reasonable to expect that $\Delta + \sigma_A$ is at approximately the same energy as the Q_y transition energy for Chl a·Pyr. Thus,

$$\Delta + \sigma_A \sim 15.02 \times 10^3 \text{ cm}^{-1} \quad (6)$$

an energy very close to the energy (15.00 × 10^3 cm^{-1}) of ϵ_+. Substituting eq 6 into the right-hand side of eq 4 gives

$$\Delta + \sigma_D \sim 14.66 \times 10^3 \text{ cm}^{-1} \quad (7)$$

an energy very close to the energy (14.69 × 10^3 cm^{-1}) of ϵ_-. We conclude that almost all of the splitting between the ϵ_+ and ϵ_- exciton transitions can be reasonably assigned to the environmental differences between the donor and acceptor Chl a molecules, and the transition density-transition density interaction energy $|T|$ must be small relative to $\sigma_A - \sigma_D$ since $|T|$ contributes little to the total splitting.

In order to provide additional experimental support for the conclusion stated above, a donor-acceptor system was sought in which Chl a functioned as a donor through the ring V keto C=O. The acceptor could not have strongly absorbing transitions in the region of the Q_y transition of Chl a. Such an acceptor system was found to be the lanthanide shift reagent, Eu(fod)$_3$. It has been shown in a previous study[40] that Eu(fod)$_3$ binds as an acceptor to the keto C=O, and in the present study it was determined that Eu(fod)$_3$ does not absorb appreciably in the Q_y region of the Chl a absorption spectrum, and therefore electronic transitions on Eu(fod)$_3$ do not mix with the Q_y transitions on Chl a through transition density-transition density interactions. A solution of ~10^{-5} M (nominal[25] concentration) Chl a in CCl_4 was titrated with Eu(fod)$_3$ until no further changes were observed upon addition of more Eu(fod)$_3$. The resulting spectrum at the end point of the titration is shown in Figure 7. It is highly significant that donor Chl a in coordination to Eu^{3+} has its Q_y transition strongly shifted to ~676 nm. This spectroscopic observation constitutes strong evidence that there is a strong environmental red shift associated with the donor role of Chl a.

Let us now turn to the question of the dipole strengths of the two exciton transitions. The ratio of the dipole strengths (D_+ and D_-) of the two exciton transitions is given by

$$D_+/D_- = \frac{1 + \cos\theta\left[\dfrac{4T^2}{(\sigma_A - \sigma_D)^2 + 4T^2}\right]^{1/2}}{1 - \cos\theta\left[\dfrac{4T^2}{(\sigma_A - \sigma_D)^2 + 4T^2}\right]^{1/2}} \quad (8)$$

where θ is the angle between the Q_y transition dipole on the donor molecule and the Q_y transition dipole on the acceptor molecule. As judged by the dipole strengths (4.8 and 4.4 D^2) of Gaussians 5 and 6 in Figure 6, $D_+/D_- \sim 1.09$. From eq 8 it follows that $D_+/D_- \sim 1$ (a) if $\cos\theta \sim 0$, or (b) if $4T^2 \ll (\sigma_A - \sigma_D)^2$. We have already reasoned that condition b holds so there is very little information left in the D_+/D_- ratio to determine θ. In the present study we did not even attempt to determine θ because of the additional problem of the sensitivity of D_+/D_- to the presence of small amounts of monomer. Specifically, monomer Chl a in CCl_4 absorbs quite near ϵ_+, and therefore Gaussian 5 in Figure 6 contains a contribution from any monomer present. If only 4.4% of the Chl a is monomeric (i.e., Chl a or Chl a·ligand species) in 10^{-5} M Chl a solution in CCl_4, then the difference (0.4 D^2) between the dipole strengths of the two Gaussians is fully accounted for.

B. Purity of Dimer Exciton States. From exciton theory for (Chl a)$_2$, the percent purity, P, of an exciton state with respect to local excitation is given by

$$P = 50\left\{1 + \left[1 + \left(\frac{\sigma_A - \sigma_D}{2T}\right)^{-2}\right]^{-1/2}\right\} \quad (9)$$

This is interpreted physically to mean that in the "+" exciton state a percent, P, of the excitation is located on the acceptor molecule and a percent, 100 − P, of the excitation is located on the donor molecule. Similarly, for the "−" exciton state a

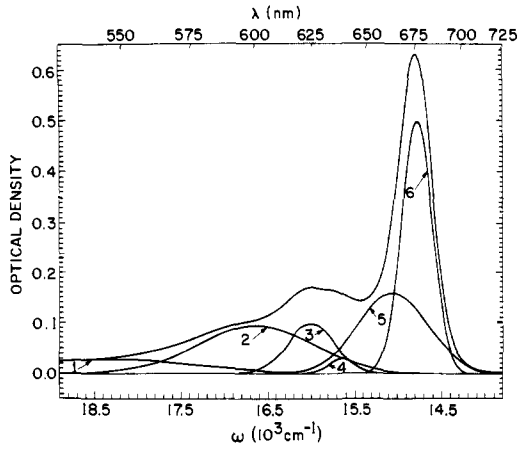

Figure 7. Visible absorption spectrum of 10^{-5} M Chl a in CCl_4 with an excess of $Eu(fod)_3$.

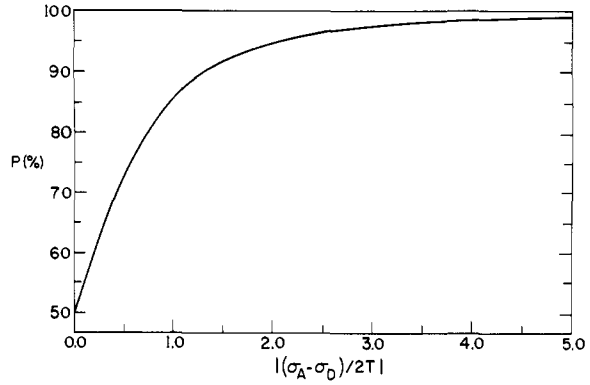

Figure 8. Purity of a dimer exciton state with respect to local excitation as a function of the absolute value of the ratio of environmental splitting over transition density splitting.

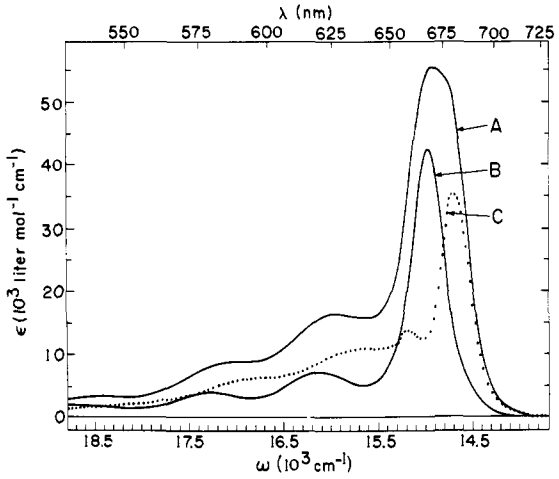

Figure 9. (A) Visible absorption spectra of chlorophyll a dimer in carbon tetrachloride. (B) Adjusted (see text) visible absorption spectrum of chlorophyll a·Pyr in carbon tetrachloride. (C) Approximate visible absorption spectrum of donor chlorophyll a (see text).

percent, P, of the excitation is on the donor molecule and a percent, $100 - P$, is on the acceptor molecule. Note that P is a function only of the ratio of the environmental splitting, $|\sigma_A - \sigma_D|$, over the transition density splitting, $|2T|$. In Figure 8 is shown a plot of P vs. $|(\sigma_A - \sigma_D)/2T|$; note that the environmental splitting is very effective at increasing P, i.e., at localizing the excitation. For example, if the environmental splitting is greater than the transition density splitting, over 85% of the excitation in the "+" exciton state is localized on the acceptor molecule and over 85% of the excitation in the "−" exciton state is localized on the donor molecule.

C. Calculation of an Approximate Absorption Spectrum for Donor Chlorophyll a. Because the "+" and "−" Q_y exciton transitions are highly localized on the acceptor and donor Chl molecules, respectively, the dimer absorption spectrum in the Q_y region is essentially the sum of a donor absorption spectrum and an acceptor absorption spectrum. It follows that if the acceptor spectrum (or a good approximation to the acceptor spectrum) were subtracted from the dimer spectrum the difference would be an approximate donor spectrum. We have adjusted the absorption spectrum of Chl a·Pyr (in CCl_4) in two ways to make it a suitable approximation to an acceptor spectrum. First, the entire spectrum was red-shifted so that the position of the narrow Gaussian component of the $Q_y(0,0)$ peak of Chl a·Pyr corresponded to the position (15.00×10^3 cm^{-1}) of the acceptor Gaussian component in the $(Chl\ a)_2$ spectrum. Next the shifted spectrum of Chl a·Pyr was scaled down so that the height of the major red peak was 42.4×10^3 l. mol^{-1} cm^{-1}, or one-half the height of the monomer spectrum. The spectrum of $(Chl\ a)_2$ in CCl_4 (spectrum A), the adjusted spectrum of Chl a·Pyr in CCl_4 (spectrum B), and the difference (spectrum C) between spectra A and B are all shown in Figure 9. Spectrum C is an approximation to the donor spectrum. The small peak at $\sim 15.20 \times 10^3$ cm^{-1} in spectrum C may be a real feature of the donor spectrum, but is probably an artifact of our analysis that arose because there is actually a small amount of monomer present in the 10^{-5} M Chl a solution for which the dimer spectrum (spectrum A) was taken. A very small amount of monomer of the order of 2% can explain the structural features in the $14.95 - 15.25 \times 10^3$ cm^{-1} region of spectrum C if the monomer is assumed to absorb at ~658 nm. It is interesting that the height of the donor peak is less than the height of the acceptor peak; compared with the acceptor spectrum there is a decrease in oscillator strength in the $Q_y(0,0)$ peak region and a substantial increase in the remainder of the spectrum.

Sauer et al.[41] have analyzed the visible absorption spectrum of Chl a in *wet* CCl_4. Because the CCl_4 was wet, a significant amount of Chl a·H_2O was surely present. An exciton theory that did not include environmental splitting was used to analyze the $Q_y(0,0)$ region of the dimer spectrum, and it was assumed that both $Q_y(0,0)$ exciton transitions in the dimer had the same spectral shape. In contrast, the results of the present study indicate that environmental splitting is quite important and the two $Q_y(0,0)$ exciton transitions (donor and acceptor) have different shapes.

D. Q_x and $Q_y(0,1)$ Regions of the Visible Absorption Spectrum. Let ϕ_A^0, ϕ_A^1, and ϕ_A^2 denote the wavefunctions for the ground electronic state (S_0), the first excited electronic state (S_1), and the second excited electronic state (S_2) of the acceptor molecule. Also, let $\chi_A^0(n)$, $\chi_A^1(n)$, and $\chi_A^2(n)$ denote the vibrational wavefunction for the nth vibrational level for a vibration in the S_0, S_1, and S_2 electronic states, respectively, of the acceptor molecule. Analogous definitions hold for donor molecule wavefunctions; only the subscript is changed from "A" to "D". We assume that the vibronic wavefunction can be represented as the product of electronic and vibrational wavefunctions, and for simplicity we will consider only the vibration most important for the vibronic coupling, i.e., the vibration that gives rise to the characteristic splitting between the (0,0) and (0,1) vibronic bands in the absorption spectrum of monomeric Chl a. The $Q_y(0,0)$ transitions that we have already considered can be represented as the following:

$$\phi_A^0\chi_A^0(0)\phi_D^0\chi_D^0(0) \rightarrow \phi_A^1\chi_A^1(0)\phi_D^0\chi_D^0(0) \quad (10)$$

$$\phi_A^0\chi_A^0(0)\phi_D^0\chi_D^0(0) \rightarrow \phi_A^0\chi_A^0(0)\phi_D^1\chi_D^1(0) \quad (11)$$

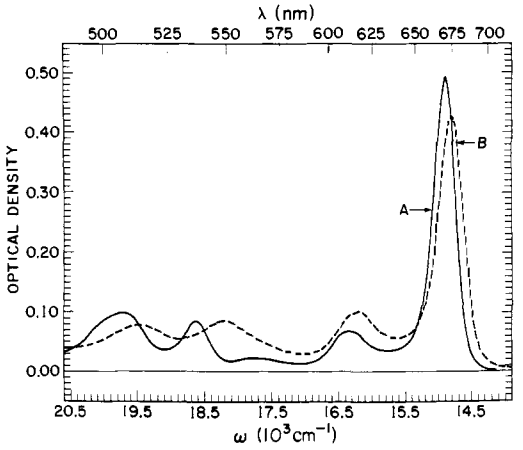

Figure 10. Visible absorption spectrum of 10^{-5} M pheophytin a in CCl_4 before (spectrum A) and after (spectrum B) addition of an excess of $Eu(fod)_3$.

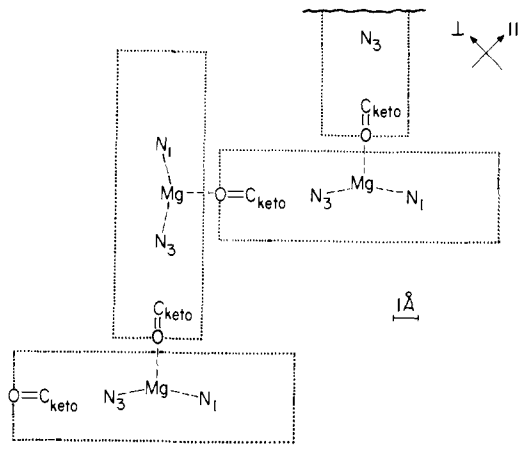

Figure 11. Structure of $(chlorophyll\ a)_n$ projected onto a plane containing the oligomer axis. All distances (see text) are drawn to scale. Arrows in the upper right-hand corner indicate directions parallel (||) and perpendicular (⊥) to the oligomer axis.

The situation becomes more complicated when considering the $Q_y(0,1)$ band in the dimer because there are four transitions that could possibly couple. These are the following:

$$\phi_A^0\chi_A^0(0)\phi_D^0\chi_D^0(0) \rightarrow \phi_A^1\chi_A^1(1)\phi_D^0\chi_D^0(0) \quad (12)$$

$$\phi_A^0\chi_A^0(0)\phi_D^0\chi_D^0(0) \rightarrow \phi_A^1\chi_A^1(0)\phi_D^0\chi_D^0(1) \quad (13)$$

$$\phi_A^0\chi_A^0(0)\phi_D^0\chi_D^0(0) \rightarrow \phi_A^0\chi_A^0(0)\phi_D^1\chi_D^1(1) \quad (14)$$

$$\phi_A^0\chi_A^0(0)\phi_D^0\chi_D^0(0) \rightarrow \phi_A^0\chi_A^0(1)\phi_D^1\chi_D^1(0) \quad (15)$$

In transitions 12 and 13 (14 and 15) the acceptor (donor) molecule is electronically excited but in transition 12 (15) the acceptor molecule is vibrationally excited and in transition 13 (14) the donor molecule is vibrationally excited. There is a total of six pairwise interaction energies among these four excited states, and these interactions can mix transitions 12 through 15. Interaction energies between 12 and 13 and between 14 and 15 are identically zero because the vibrational overlap (Franck-Condon factors) part of the interaction energy integrals are zero, i.e.,

$$\langle\chi_A^1(1)|\chi_A^1(0)\rangle = \langle\chi_D^0(0)|\chi_D^0(1)\rangle = \langle\chi_A^0(0)|\chi_A^0(1)\rangle = \langle\chi_D^1(1)|\chi_D^1(0)\rangle = 0 \quad (16)$$

Because the difference between the environmental energy shifts of the Q_y transition of donor and acceptor is substantially greater than the transition density splitting, the mixing is small between transitions differing as to the molecule electronically excited. Thus, mixing between 12 and either 14 or 15, and between 13 and either 14 or 15, is small. It follows that the dimer transitions should be largely unmixed 12 through 15. Because of vibrational overlap factors (eq 16) the transition moments for transitions 13 and 15 are zero. Therefore *only* transitions 12 and 14 should be observed in the $Q_y(0,1)$ region of the dimer spectrum. Because twice the standard deviation of the $Q_y(0,1)$ Gaussian (see Gaussian 3, Figure 2) in the monomer spectrum is greater than the donor-acceptor environmental difference (310 cm^{-1}) the acceptor $Q_y(0,1)$ (i.e., transition 12) and donor $Q_y(0,1)$ (i.e., transition 14) Gaussians add together to form a single broad peak in the dimer spectrum. The center of this broad peak (15.99×10^3 cm^{-1}) is 1.15×10^3 cm^{-1} to the blue of the average position (14.84×10^3 cm^{-1}) of the two narrow Gaussian components of the $Q_y(0,0)$ transitions. This energy separation (1.15×10^3 cm^{-1}) between the $Q_y(0,0)$ and $Q_y(0,1)$ transitions in the dimer is in excellent agreement with the energy difference (1.16×10^3 cm^{-1}) between the $Q_y(0,0)$ and $Q_y(0,1)$ transitions in the monomer. In conclusion, the $Q_y(0,1)$ region of the dimer spectrum can be satisfactorily explained on the basis of transition 12 occurring at 16.14×10^3 cm^{-1} (620 nm) and transition 14 occurring at 15.84×10^3 cm^{-1} (631 nm) (environmental splitting of 3.1×10^2 cm^{-1}) in such a way that their rather broad peaks overlap to give a single even broader peak centered at 15.99×10^3 cm^{-1} (625 nm).

A comparison of the approximate donor and acceptor spectra in Figure 9 with the monomer spectra in Figures 2-4, indicates that Q_x may be red-shifted farther than Q_y by the donor interaction. In particular, there is a small peak at $\sim 15.65 \times 10^3$ (639 nm) cm^{-1} in the $Eu(fod)_3$·Chl a spectrum, and that peak may be $Q_x(0,0)$; the $Q_x(0,1)$ region seems to be much diminished compared with the same region of Chl a monomer spectra, and this may reflect a shift of the entire Q_x transition to the red. We have indirect evidence that bears on the question of the behavior of Q_x upon donor interaction. In particular, for monomeric 10^{-5} M Pheophytin a (Pheo a) in CCl_4 the $Q_y(0,0)$ peak is at 14.91×10^3 cm^{-1} (671 nm) and the $Q_x(0,0)$ peak is at 18.63×10^3 cm^{-1} (537 nm), and this spectrum is shown in Figure 10 as spectrum A. For 10^{-5} M Pheo a with an excess of $Eu(fod)_3$ in CCl_4 the $Q_y(0,0)$ peak is at 14.82×10^3 cm^{-1} (675 nm) and the $Q_x(0,0)$ peak is at 18.19×10^3 cm^{-1} (550 nm). Thus the Q_y transition red shifts by 9×10^1 cm^{-1} in the donor to Eu^{3+} while the Q_x red shifts by 4.4×10^2 cm^{-1}. We conclude that as in the case of Pheo a the Q_x transition of Chl a may be red-shifted substantially more than the Q_y transition in the donor.

VII. Absorption Spectra of Chlorophyll a Oligomers in *n*-Octane

Chl a oligomers are most likely found formed via a continuation of the donor-acceptor interactions that bind the Chl a dimer. A schematic representation of such an oligomer structure is shown in Figure 11. The chlorophyll molecule at one end is acceptor only, the molecule at the other end is donor only, and all the molecules in between are both donor and acceptor (i.e., donor-acceptor). The distances in Figure 11 were estimated by use of distances found in the Strouse et al. x-ray crystallographic structure[26] of ethyl chlorophyllide a·$2H_2O$. For example, the Mg has been placed 0.4 Å out of the N(I)-N(II)-N(III)-N(IV) plane in the direction of the intermolecular coordination bond, and the length of the Mg- - -O coordination bond has been set at 2.1 Å. The projected intramolecular distances were taken directly from the crystal structure. The dotted lines surrounding each Chl a molecule represent approximate van der Waals radii of 1.8 Å, one-half the distance between macrocycle planes in the Strouse crystal structure.

We have studied the visible absorption spectrum of Chl a in dry *n*-octane as a function of nominal[25] Chl a concentration. The visible absorption spectrum of 1.3×10^{-5} M (spectrum A), 1.3×10^{-4} M (spectrum B), 1.3×10^{-3} M (spectrum C), and 1.5×10^{-2} M (spectrum D) Chl a in *n*-octane are shown in Figure 12. Note that a set of Gaussians with very similar positions and standard deviations deconvolute the spectra for all four concentrations. The biggest change in the spectra with increasing concentration is the increase in the contribution of Gaussian 6 at the expense of Gaussian 5. By analogy to the assignments for $(\text{Chl a})_2$ we assign Gaussian 5 to the acceptor-only molecule at one end of the oligomer, and Gaussian 6 is assigned to the donor-only molecule at the other end of the oligomer and to all the donor-acceptor molecules in the middle. Estimates for average chain length, l_{ave}, can be obtained by comparison of the dipole strengths of Gaussians 5 and 6; the average chain length is the ratio of the sum of the dipole strengths for Gaussians 5 (D_5) and 6 (D_6) over the dipole strength for Gaussian 5 alone:

$$l_{ave} = \frac{D_5 + D_6}{D_5} \qquad (17)$$

The average oligomer lengths are computed using eq 17 to be 2.0, 2.2, 3.4, and 4.9 for Chl a concentrations of 1.3×10^{-5}, 1.3×10^{-4}, 1.3×10^{-3}, and 1.5×10^{-2} M, respectively. An average oligomer length of ~5 for 1.5×10^{-2} M Chl a in *n*-octane is consistent with the vapor-phase osmometry results of Ballschmiter et al.[33] who found that the average oligomer length for 10^{-2} M Chl a in *n*-hexane was ~6. At the three lower concentrations in Figure 12 Gaussians 5 and 6 are found at 15.09×10^3 cm^{-1} (663 nm) and 14.76×10^3 cm^{-1} (678 nm), respectively. At the 1.5×10^{-2} M concentration Gaussians 5 and 6 are at 15.06×10^3 cm^{-1} (664 nm) and 14.74×10^3 cm^{-1} (678 nm), respectively, only very slightly red-shifted from their positions at the lower concentrations. For $(\text{Chl a})_2$ in CCl_4, the Gaussians 5 and 6 are at (Table III) 15.00×10^3 cm^{-1} (667 nm) and 14.69×10^3 cm^{-1} (681 nm), respectively. Thus relative to CCl_4, the average position of Gaussians 5 and 6 in *n*-octane is blue-shifted by 8×10^2 cm^{-1} from 14.84×10^3 cm^{-1} to 14.92×10^3 cm^{-1}, and the splitting is 3.3×10^2 cm^{-1} in *n*-octane compared with 3.1×10^2 in CCl_4. It is possible to determine whether this blue shift is due to a different dimer conformation in the two solvents or just a bulk solvent environmental shift. We have determined the bulk solvent environmental shift by comparison of the position of the absorption of Chl a·Pyr in *n*-octane and CCl_4. Pyridine is very effective at disaggregating Chl a dimer to Chl a·Pyr; small amounts of pyridine were added to Chl a solutions in CCl_4 and *n*-octane until the visible absorption spectrum was clearly that of a monomeric species. The narrow Gaussian component in the visible absorption spectrum of Chl a·Pyr is at 15.02×10^3 cm^{-1} in CCl_4 and at 15.10×10^3 cm^{-1} in *n*-octane, a blue shift of 8×10^2 cm^{-1} in *n*-octane compared with CCl_4. Thus the blue shift of $(\text{Chl a})_2$ in *n*-octane compared with CCl_4 is entirely a bulk solvent environmental shift.

The width of Gaussian 5 in the spectrum of $(\text{Chl a})_n$ in *n*-octane is nearly concentration independent (δ 140 ± 5 cm^{-1}) while the width of Gaussian 6 increases slightly from δ 134 cm^{-1} at 1.3×10^{-5} M to δ 159 cm^{-1} at 1.5×10^{-2} M. These widths compare with the widths of 156 and 145 cm^{-1} found for Gaussians 5 and 6 in CCl_4. The spectrum of $(\text{Chl a})_2$ in CCl_4 does not show two separate maxima (Figure 6) corresponding to donor and acceptor; on the other hand, because the donor and acceptor Gaussians are slightly narrower and slightly farther apart in *n*-octane, the donor and acceptor peaks appear as separate maxima (spectrum A, Figure 12).

A. Exciton Theory: Chlorophyll a Oligomers in *n*-Octane. It is reasonable to expect that adjacent molecules in $(\text{Chl a})_n$ have an orthogonal or nearly so orientation (as in Figure 11)

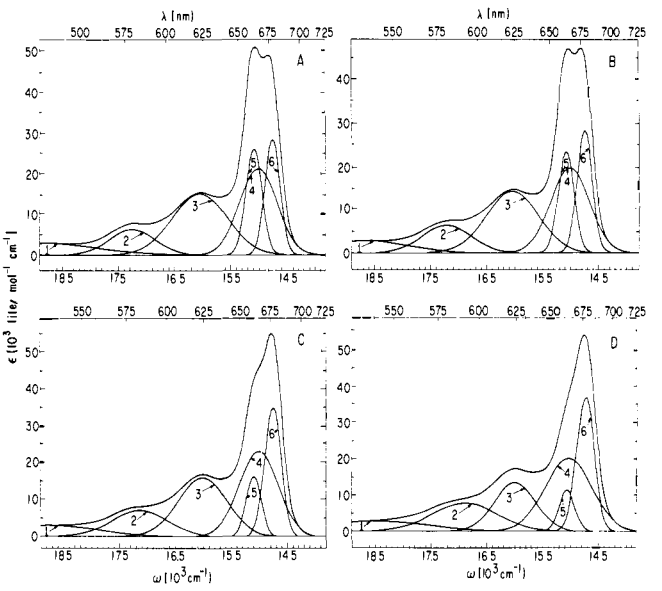

Figure 12. Visible absorption spectra of chlorophyll a oligomers in *n*-octane at nominal[25] chlorophyll a concentrations of 1.3×10^{-5} M (spectrum A), 1.3×10^{-4} M (spectrum B), 1.3×10^{-3} M (spectrum C), and 1.5×10^{-2} M (spectrum D).

so as to optimize the directionality of the keto C=O- - -Mg coordination bond and to minimize overlap repulsions. In this arrangement, the transition density-transition density interaction energy between adjacent molecules will be zero or very small. The positions and relative dipole strengths for the exciton transitions in an infinitely long $(\text{Chl a})_n$ chain are readily computed. The infinite chain is viewed as a one-dimensional crystal with two molecules per unit cell (vertical Chl a molecules and horizontal Chl a molecules; Figure 11). The dipole strength of the $Q_y(0,0)$ transition is 16.7 D^2 (the sum of the dipole strengths of Gaussians 4 and 5, Table II), and we take the direction of the transition dipole to be along N(I)-N(III).[21] The position of the donor-acceptor absorption is at 14.76×10^3 cm^{-1} (678 nm) after environmental shifting. The interaction of the transition densities of all the vertical Chl a molecules (or all the horizontal Chl a molecules) results in a manifold of exciton transitions 1.2×10^2 cm^{-1} wide ranging from 14.70×10^3 to 14.82×10^3 cm^{-1} (680 to 675 nm) and centered at 14.76×10^3 cm^{-1}. However, the red-most transition has all the dipole strength. The coupling of horizontal to vertical Chl a molecules further widens the exciton transition manifold so that the total width is 2.0×10^2 cm^{-1} and the manifold runs from 14.66×10^3 cm^{-1} (682 nm) to 14.86×10^3 cm^{-1} (673 nm). All of the dipole strength goes equally to just two exciton transitions, one at 14.66×10^3 cm^{-1} (682 nm) polarized along the axis of the chain ($\parallel$, Figure 11) and the other at 14.74×10^3 cm^{-1} (678 nm) polarized perpendicular to the axis of the chain ($\perp$, Figure 11). These two transition peaks would be expected to be Gaussian and have a width nearly the same as that of monomer Chl a (i.e., $\delta \sim 140$ cm^{-1}). Because the separation of the Gaussians (i.e., 120 cm^{-1}) is less than twice the standard deviation of the Gaussians (i.e., less than 280 cm^{-1}), the sum of the two Gaussians has a single maximum centered at 14.70×10^3 cm^{-1} (680 nm) for excitation by unpolarized light. If the oligomer is excited by plane polarized light with the oscillating electric vector of the light parallel (see $\parallel$ arrow, Figure 11) to the axis of the chain, then the absorption peak will be at 682 nm; on the other hand, if the chain is excited by plane polarized light with the electric vector of the light perpendicular (see $\perp$ arrow, Figure 11) to the chain, the absorption peak will be at ~678 nm.

B. Implications for Energy Transfer in Antenna Chlorophyll a. It has been previously shown[14] that for plant species con-

taining only Chl a there is a striking similarity between their visible absorption spectra and the visible absorption spectra of Chl a oligomers for concentrated Chl a solutions in aliphatic solvents. This observation led to the proposal that antenna Chl a in vivo is largely in the form of Chl a oligomers in hydrophobic regions of the chloroplast. Beddard and Porter[42] have proposed that chlorophyll molecules in the antenna are monomeric, close together, and separated by strongly coordinated molecules. Such a model can be made consistent with the observed[14] absorption spectrum for well-separated monomers (maximum at 659-671 nm depending upon ligand, coordination state, and bulk solvent) and antenna chlorophyll (maximum at ~678 nm) only if there is a substantial amount of long range ordering of the monomer Q_y transition dipoles. However, as far as we know there is no experimental evidence for such long range ordering in the antenna. We conclude that the chlorophyll oligomers are still the best model for the state of chlorophyll in the antenna. The various antenna models have been discussed in more detail elsewhere.[43]

The exciton calculation for an infinite $(\text{Chl a})_n$ chain (section VII.A.) leads to a proposal for the mechanism of energy transfer along $(\text{Chl a})_n$. The maximum transition density interaction in $(\text{Chl a})_n$ is found for the infinite chain, and for this case the transition density interaction energy between a particular molecule and all the other molecules in the chains is 100 cm^{-1}. Such a weak interaction should lead[44] to excitation energy migration along $(\text{Chl a})_n$ via the Förster[45] energy-transfer mechanism. In the $(\text{Chl a})_n$ model for antenna chlorophyll (i) the photon is absorbed into a delocalized exciton state involving coherent excitations on many Chl molecules, (ii) the coherence is quickly broken by intermolecular collisions, (iii) the excitation energy diffuses along the antenna as if the excitation on each Chl molecule diffuses independently, until (iv) a trap is reached. Each Chl oligomer may serve more than one trap. The most probable energy transfers along a $(\text{Chl a})_n$ chain are to second or third nearest neighbors because there is little or no transition dipole coupling energy between nearest neighbors and the R^{-6} dependence of the transfer rate makes transfers beyond third neighbors less likely than transfers to second or third nearest neighbors. Because $(\text{Chl a})_n$ is only weakly fluorescent the rate of fluorescence quenching must be fast compared with the fluorescence rate. We believe that the rate of energy transfer in the oligomer is fast compared with the rate of fluorescence quenching, and therefore the low fluorescence yield of $(\text{Chl a})_n$ does not imply absence of energy transfer. The similarity of the visible absorption spectra and low fluorescence yields between in vivo antenna chlorophyll and $(\text{Chl a})_n$ along with the suitability of the oligomer for energy transfer makes the oligomer, in our view, an attractive model for the ~680 nm component of in vivo antenna chlorophyll.

Acknowledgments. We thank W. Svec and B. Cope for the preparation of the chlorophyll a used in this work and A. Zielen for his assistance with the spectral deconvolution program. We acknowledge M. Dunetz for his efforts in preliminary investigations related to this work. We give a special thanks to Dr. Pill-Soon Song for his comments and criticisms after reading this manuscript and for making his data available to us prior to publication. We thank Dr. R. S. Knox, Sir George Porter, and Dr. G. R. Seely for comments and criticisms.

References and Notes

(1) This work was performed under the auspices of the United States Energy Research and Development Administration.
(2) Participant in the Argonne Thesis Program, administered by the Argonne Center for Educational Affairs.
(3) R. Emerson and W. Arnold, *J. Gen. Physiol.*, **15**, 391-420 (1931-32).
(4) R. Emerson and W. Arnold, *J. Gen. Physiol.*, **16**, 191-205 (1932-33).
(5) R. K. Clayton, *Adv. Chem. Phys.*, **19**, 353-378 (1971).
(6) J. J. Katz and J. R. Norris in "Current Topics in Bioenergetics", Vol. 5, Academic Press, New York, N.Y., 1973, pp 41-75.
(7) R. K. Clayton, *Annu. Rev. Biophys. Bioeng.*, **2**, 131-156 (1973).
(8) J. A. Prins, *Nature*, **134**, 457-458 (1934).
(9) G. P. Gurinovich, A. N. Sevchenko, and K. N. Solov'ev, *Sov. Phys. Usp. (Engl. Transl.)*, **6**, 67-105 (1963).
(10) G. P. Gurinovich, A. N. Sevchenko, and K. N. Solov'ev, "Spectroscopy of Chlorophyll and Related Compounds", A.E.C. Translation Series, AEC-tr-7199, 1968.
(11) C. Weiss, *J. Mol. Spectrosc.*, **44**, 37-80 (1972).
(12) J. J. Katz in "Inorganic Biochemistry", G. Eichhorn, Ed., Elsevier, Amsterdam, 1972, pp 1022-1066.
(13) J. J. Katz, *Naturwissenschaften*, **60**, 32-39 (1973).
(14) T. M. Cotton, A. D. Trifunac, K. Ballschmiter, and J. J. Katz, *Biochim. Biophys. Acta*, **368**, 181-198 (1974).
(15) J. R. Norris, H. Scheer, and J. J. Katz, *Ann. N.Y. Acad. Sci.*, **244**, 260-280 (1975).
(16) J. J. Katz, L. L. Shipman, T. M. Cotton, and T. R. Janson in "The Porphyrins", D. Dolphin, Ed., in press.
(17) L. L. Shipman, J. R. Norris, and J. J. Katz, *J. Phys. Chem.*, **80**, 877-882 (1976).
(18) H. H. Strain and W. Svec in "The Chlorophylls", L. P. Vernon and G. R. Seely, Ed., Academic Press, New York, N.Y., 1966, pp 21-66.
(19) P. H. Hynninen, *Acta Chem. Scand.*, **27**, 1487-1495 (1973).
(20) W. C. Davidon, "Variable Metric Method for Minimization", ANL-5990 (Rev. 2) 1966, Argonne National Laboratory.
(21) P. S. Song, T. A. Moore, and M. Sun, *Adv. Food Res. Suppl.*, **3**, 33-74 (1972).
(22) The oscillator strength, f (unitless), is given by $(10^3 2^{1/2} mc^2 \delta \epsilon_0 \ln 10)/(\Pi^{1/2} e^2 Nn)$ and the dipole strength (D^2) is given by $[(3he^2 10^{36})/(8\Pi^2 mc)](f/\omega_0)$, where m is the electron mass, c is the speed of light, e is the electron charge, N is Avagodro's number, h is Planck's constant, and n is the index of refraction. See eq 1 for the definition of the Gaussian parameters δ, ϵ_0, and ω_0.
(23) J. Fünfschilling and D. F. Williams, *Photochem. Photobiol.*, **22**, 151-152 (1975).
(24) W. Siebrand, *J. Chem. Phys.*, **40**, 2223-2230 (1964).
(25) By "nominal Chl a concentration" we mean the Chl a monomer concentration that would obtain if all the Chl a species were converted to monomeric species.
(26) H.-S. Chow, R. Serlin, and C. E. Strouse, *J. Am. Chem. Soc.*, **97**, 7230-7237 (1975).
(27) T. A. Evans and J. J. Katz, *Biochim. Biophys. Acta*, **396**, 414-426 (1975).
(28) P. J. McCartin, *J. Phys. Chem.*, **67**, 513-514 (1963).
(29) G. R. Seely and R. G. Jensen, *Spectrochim. Acta*, **21**, 1835-1845 (1965).
(30) Private communication from Pill-Soon Song.
(31) S. Freed and K. M. Sancier, *Science*, **114**, 275-276 (1951).
(32) A. N. Sevchenko, K. N. Solov'ev, V. A. Mashenkov, S. F. Shkirman, and A. P. Losev, *Sov. Phys.-Dokl. (Engl. Transl.)*, **12**, 787-789 (1968).
(33) K. Ballschmiter, K. Truesdell, and J. J. Katz, *Biochim. Biophys. Acta*, **184**, 604-613 (1969).
(34) J. J. Katz, G. L. Closs, F. C. Pennington, M. R. Thomas, and H. H. Strain, *J. Am. Chem. Soc.*, **85**, 3801-3809 (1963).
(35) A. F. H. Anderson and M. Calvin, *Arch. Biochem. Biophys.*, **107**, 251-259 (1964).
(36) M. Henry and J.-P. Leicknam, *Colloq. Int. C. N. R. S.*, **No. 191**, 317-333 (1970).
(37) J. J. Katz, T. R. Janson, A. G. Kostka, R. A. Uphaus, and G. L. Closs, *J. Am. Chem. Soc.*, **94**, 2883-2885 (1972).
(38) J. J. Katz and T. R. Janson, *Ann. N.Y. Acad. Sci.*, **206**, 579-603 (1973).
(39) L. L. Shipman, T. R. Janson, G. J. Ray, and J. J. Katz, *Proc. Natl. Acad. Sci. U.S.A.*, **72**, 2873-2896 (1975).
(40) A. D. Trifunac and J. J. Katz, *J. Am. Chem. Soc.*, **96**, 5233-5240 (1974).
(41) K. Sauer, J. R. Lindsay-Smith, and A. J. Schultz, *J. Am. Chem. Soc.*, **88**, 2681-2688 (1966).
(42) G. S. Beddard and G. Porter, *Nature*, **260**, 366-367 (1976).
(43) J. J. Katz, J. R. Norris, and L. L. Shipman, *Brookhaven Symp. Biol.*, **28**, in press.
(44) V. M. Kenkre and R. S. Knox, *Phys. Rev. Lett.*, **33**, 803-806 (1974).
(45) Th. Förster, "Modern Quantum Chemistry", O. Sinanoğlu, Ed., Academic Press, New York, N.Y., 1965, pp 93-137.